Liquid Crystals
Publication details, including instructions for authors and subscription information:
http://www.informaworld.com/smpp/title~content=t713926090

Spatial dispersion in chiral liquid crystals. Effects of higher orders

E. Demikhov[ab]; H. Stegemeyer[a]
[a] Institute of Physical Chemistry, University Paderborn, Paderborn, Germany [b] Institute of Solid State Physics, Russian Academy of Sciences, Chernogolovka

To cite this Article Demikhov, E. and Stegemeyer, H.(1993) 'Spatial dispersion in chiral liquid crystals. Effects of higher orders', Liquid Crystals, 14: 6, 1801 — 1830
To link to this Article: DOI: 10.1080/02678299308027717
URL: http://dx.doi.org/10.1080/02678299308027717

LIQUID CRYSTALS, 1993, VOL. 14, NO. 6, 1801–1830

Spatial dispersion in chiral liquid crystals
Effects of higher orders

by E. DEMIKHOV*† and H. STEGEMEYER
Institute of Physical Chemistry, University Paderborn,
POB 1621, D-4790 Paderborn, Germany

Spatial dispersion effects in chiral liquid crystals are reviewed. New spatial dispersion phenomena are observed in the vicinity of the Bragg reflection wavelength—an anomaly of the refractive index and an optical anisotropy of the cubic blue phases. These effects can be explained by taking into account the spatial dispersion correction of the dielectric tensor of the medium of higher orders in the ratio of the light wave vector to the structural wave vector of chiral phases.

1. Introduction

There is a well known analogy between the optics of chiral liquid crystals and common crystalline solids. General consideration of crystallo-optics takes into account effects of frequency dispersion of the dielectric tensor as well as effects of its spatial dispersion [1]. Frequency dispersion is combined with intrinsic electronic periodical motions in the substance and describes peculiarities of the optical constants in the vicinity of electronic absorption bands. By taking into account spatial dispersion, we consider the fact that the polarization vector **P** at a given point is determined by the electric field not only at that point, but also in the vicinity of the point. This leads to a dependence of the dielectric tensor on the spatial coordinate (wave vector). The spatial dispersion contribution is determined by the ratio a/λ, where a is the period of the system and λ is the wavelength of light. Therefore spatial dispersion effects give information about the local structure of the medium, which is particularly important for liquid crystals. In solid states, spatial dispersion effects are small because $a \ll \lambda$, but there is a class of phenomena (girotropy), which can be explained only by taking into account the spatial dispersion contribution.

In phases without a centre of symmetry, such as chiral liquid crystals, the strongest spatial dispersion effect is found for their optical activity, which is an effect of first order in (a/λ). In non-girotropic media, spatial dispersion is of the order of (a/λ) and therefore essentially smaller. Well known spatial dispersion effects for non-girotropic solid crystals are the optical anisotropy and the additional light waves of cubic crystals (see [1]). In our experiments, we have succeeded in observing spatial dispersion effects of higher orders in strongly girotropic liquid crystals. We have investigated perfect monodomain samples of blue phases, but this approach is general for all chiral liquid crystals. In the case of chiral liquid crystals, spatial dispersion effects can be observed in ordered phases (cholesteric and blue phases) [2–3] or in the pretransitional region in the isotropic phase, where a means the correlation radius of orientational fluctuations [4–9].

*Author for correspondence.
†On leave of absence from the Institute of Solid State Physics, Russian Academy of Sciences, 142432 Chernogolovka.

0267–8292/93 $10·00

The blue phases of liquid crystals are well suited for the investigation of spatial dispersion [12–16]. Blue phases appear in highly chiral liquid crystals in the vicinity of the point of absolute instability of the isotropic liquid. A phase diagram of the blue phases (BPs) for pure cholesteryl alkanoates is shown in figure 1 [17]. The appearance and methods of investigation of BPs are, in important points, analogous to the solid state. But, unlike solid crystals, in the case of blue phases there is only a long or short range orientational order. Nothing is known about positional order in the blue phases. Consequently, well-shaped single crystals of the BPI and BPII have been grown [18–21]. The reconstruction of the monocrystal shape from the experiments [18–19] is given in figure 2. Crystallographic analysis of observable growth forms of BPI and BPII makes it possible to determine their space groups [18–21]. Lattice constants of the blue phases correspond to the visible region of the spectrum of electromagnetic waves. The most powerful experimental methods for the structural investigation of blue phases are analogues of the X-ray structure analysis of solid crystals with visible light—the energy dispersion method [22–25] and Kossel diagrams [26–28]. In contrast to the diffraction in the X-ray spectral region, it is possible to get additional structural information in the visible region by means of polarization measurements. Figure 3 shows typical energy dispersion spectra (in reflection) of blue phases I, II and III. Reflection spectra of BPI and BPII consist of several diffraction lines, corresponding to wave vectors of reciprocal space with cubic symmetry. Blue phases I and II possess three dimensional orientational order with cubic space groups O^8 ($I4_132$) and O^2 ($P4_232$), respectively. Structures of the BPI and BPII have been described in [29–31] as three dimensional periodical packing of double twist cylinders (see figure 4). In double twist cylinders, the director is rotated around two axes—the axis of the double twist cylinder and the radius-vector perpendicular to the cylinder axis. On the boundary between different double twist cylinders, defect lines occur, which are positioned in space in accordance with the symmetry group. Blue phase III reflection spectra show a broad line typical for amorphous systems [25, 32, 33]. The symmetry group describing the local order of BPIII is still under discussion [33–37]. Recent theoretical and experimental results give

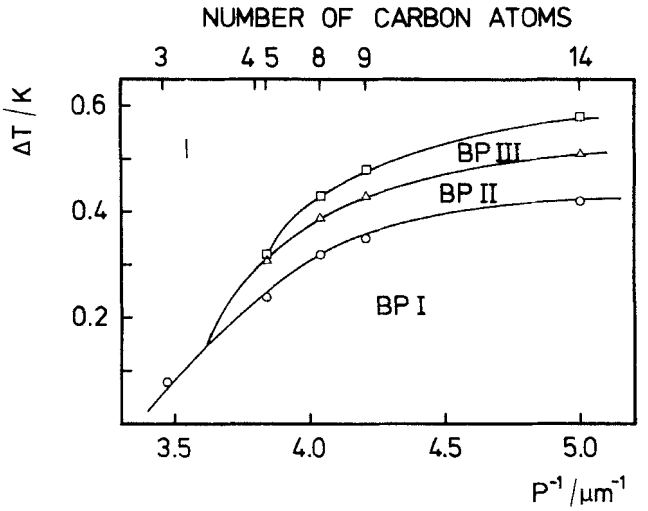

Figure 1. Temperature intervals of the stability of the blue phases versus reciprocal cholesteric pitch of pure cholesteryl alkanoates (from P. J. Collings *et al.* [17]).

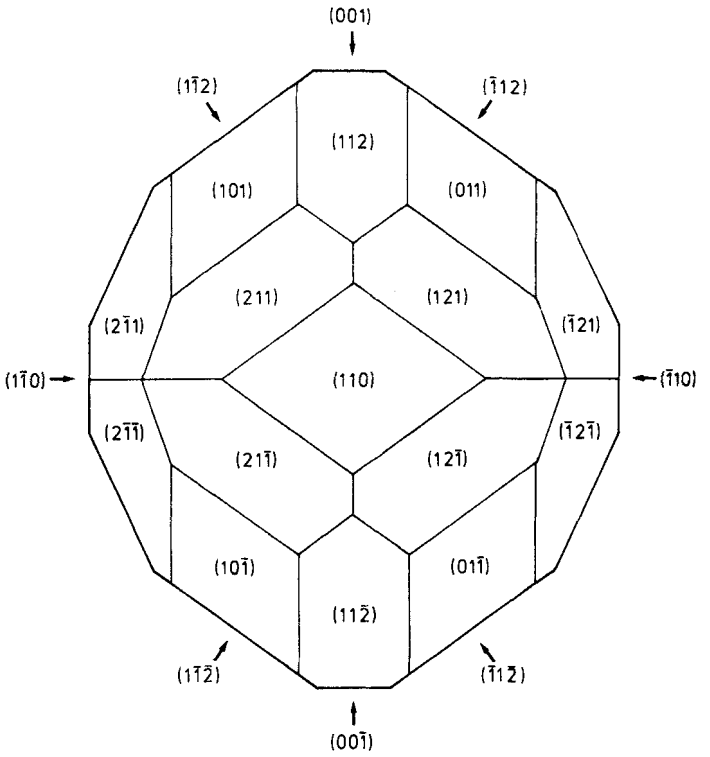

Figure 2. Reconstruction of the simple form of the monocrystals of BPs from [18, 19].

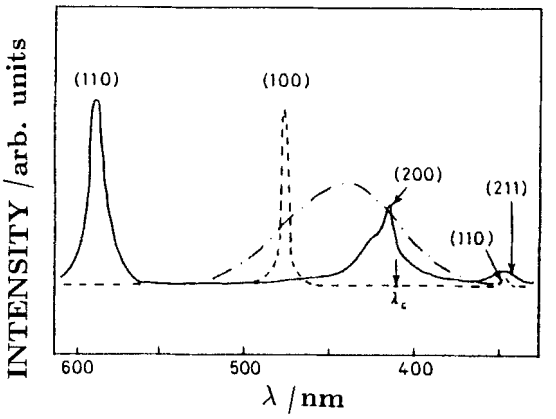

Figure 3. Energy dispersion spectra for the blue phases of the CN–CC mixture (90 : 10). ——, BPI (85·97°C); – – –, BPII (86·23°C); .–.–.–, BPIII (86·33°C) [32].

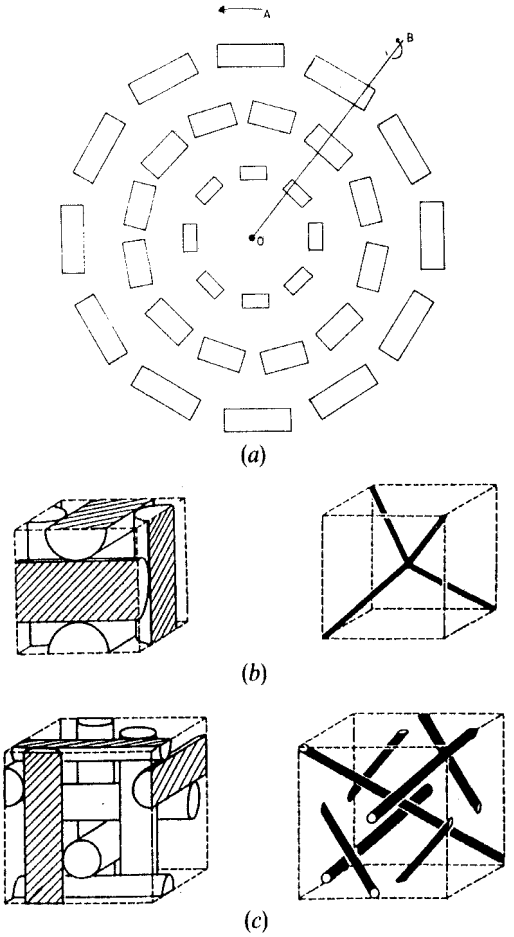

Figure 4. (*a*) Double twist cylinder cross-section perpendicular to its axis; projections of the director are shown; (*b*) double twist cylinder packing and defect line location for the space symmetry group (O^2); (*c*) analogue for the space group (O^8). ((*b*) and (*c*) are taken from the paper of E. Dubois-Violette and B. Pansu [31]).

evidence that BPIII can exhibit an icosahedral structure of the director field [38] with the ratio of basic harmonics 1 : 1·17. Figure 5 shows the asymmetrical line shape of the Bragg reflection of BPIII in a mirror cell with a shoulder at the short wavelength side and the results of fitting of this curve by a sum of two gaussians. The best fitting corresponds to a ratio of $1{\cdot}15 \pm 0{\cdot}03$ of the maximal wavelengths of gaussians. The blue phases I and II show qualitatively different line shapes. This result contradicts conclusions based on measurements of the line shape-electric field dependence in the BPIII [35].

The relation of the lattice period of the blue phases to the wavelength of light is of the order of unity. Such a drastic change in the periodicity of the system gives qualitively new possibilities for observation of spatial dispersion effects with respect to the solid state. This paper is arranged in the following manner: in § 2, we review known spatial dispersion effects in chiral liquid crystals. In § 3 we present experimental results on spatial dispersion effects of higher orders (cholesteric and blue phases) and give a possible theoretical description of it.

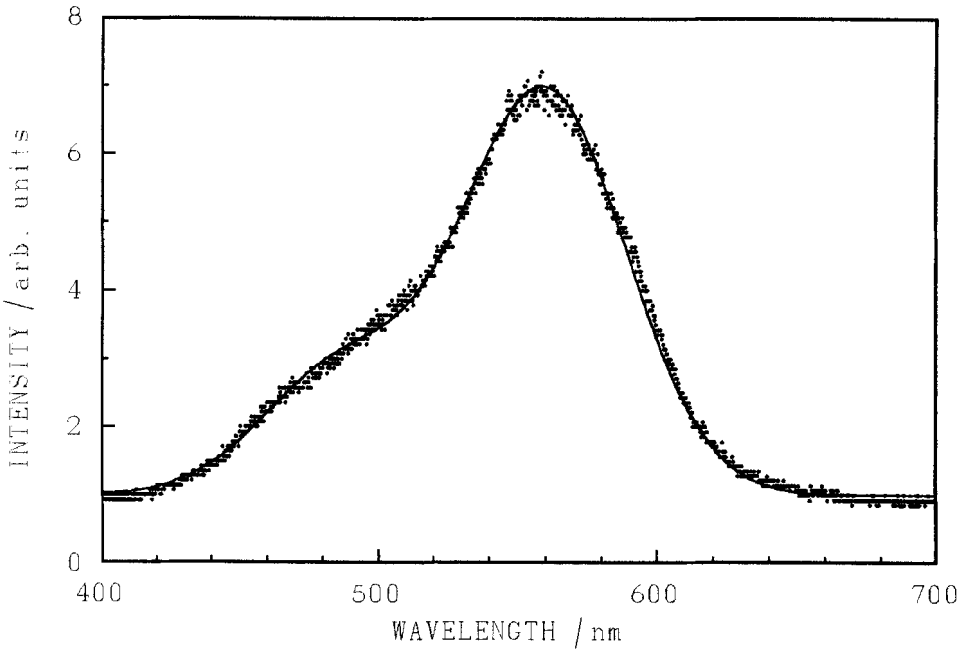

Figure 5. Selective reflection of BPIII of the mixture consisting of 18 wt% CE1, 27 wt% CE2 and 55 wt% M18 in a mirror cell with strong boundary conditions. Sample thickness $d = 30\ \mu m$. The solid line is the result of mean-square fitting of experimental data with a sum of two gaussians.

2. Optical activity

2.1. *Optical activity in the isotropic liquids of highly chiral liquid crystals*

Unusual physical properties of short pitch chiral liquid crystals in the vicinity of the point of absolute instability of the isotropic liquid have been the subject of recent theoretical and experimental investigations [4–11]. Fundamental interest in these phenomena is combined with the fact that the phase transition from the isotropic liquid in short pitch liquid crystals is nearly of second order. It is a reflection of the success of the Landau–de Gennes theory of phase transitions that it describes both precritical phenomena and the properties of the blue phases. In accordance with this general concept, long range order in BPI and BPII, as well as short range order in BPIII and the isotropic liquid can be described in terms of five structural eigenmodes. The blue phases possess a long range order with cubic symmetry (BPI and BPII) or an amorphous structure (BPIII). For the blue phases, these modes can be regarded as independent structural components of the order parameter. For the isotropic liquid, these modes describe fluctuational excitations of local order with helical (conical and spiral mode) and nematic structures [10–11]. BPIII takes an intermediate position between the ordered blue phases I and II and the isotropic liquid. The order parameter of BPIII is not equal to zero [39] and heat capacity measurements [40] show that the transition enthalpy for the phase transition isotropic liquid–BPIII is larger than those for the phase transitions BPIII–BPII, BPII–BPI, BPI–cholesteric. On the other hand, BPIII has only short range order and can be considered as a liquid with large correlation length (about 2–3 chiral periods) [25]. The phase transition isotropic liquid–BPIII can be regarded as the first example of a liquid–liquid phase transition in one-component systems. Hence, investigations of pretransitional phenomena in the isotropic liquids of

highly chiral liquid crystals are very important with regard to understanding the nature of this phase transition.

Measurements of the optical activity give the most instructive information about orientational correlations in the isotropic liquid. This is possible because of the fact that one can investigate the pure fluctuation contribution, combined with structural modes, describing the phase transition to the blue phases. The effect of pretransitional optical rotation of the plane of polarization of light has, for the first time, been observed in the isotropic liquid [4]. The non-monotonous behaviour of optical activity in the isotropic liquid in the vicinity of the phase transition to the blue phases has been found for the first time in [5] (see figures 6 and 7). The effect of pretransitional optical activity in the isotropic and the smectic A phases of ferroelectric liquid crystals was initially observed and theoretically explained in [6] (see figure 8). Further investigations of this effect [27–29] have shown the possibility of determining the correlation lengths of the chiral fluctuation modes and the coefficients of the Landau–de Gennes theory.

A theoretical description of the effect of non-monotonous behaviour of the rotation of the plane of polarization of light in the isotropic liquid has been developed [10, 41–43]. The fitting procedure of [8] has shown excellent agreement between theory and experiment. We summarize, in the following, important theoretical relations obtained earlier in the case of the pretransitional temperature effects. We present an extension of this theory to describe a pressure induced inversion of the gradient of optical activity in the isotropic liquid, recently observed in [44–45]. Then, we shall illustrate the facilities of our fitting procedure using an example of new experimental results from [45]. In the following, we use the notations common for the Landau theory of blue phases. Critical properties of the isotropic liquid and structures of the blue phases are described by the free energy Landau–de Gennes function. The Landau theory describes, in the case of blue phases, the condensation of waves of the orientational order parameter ε_{ij} (the anisotropic part of the dielectric tensor)

$$\varepsilon_{ij} = \varepsilon^d_{ij} - \tfrac{1}{3} Sp(\varepsilon^d_{ij})\delta_{ij}. \tag{1}$$

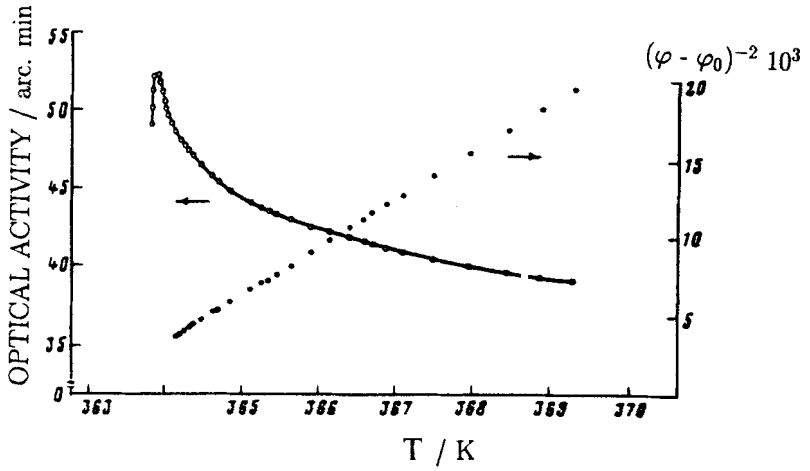

Figure 6. Optical activity of cholesteryl nonanoate in the isotropic liquid near the phase transition into BPII (○); specimen thickness $d = 2$ mm, $\lambda = 633$ nm, ●—the dependence $(\psi - \psi_0)^{-2}$ [5].

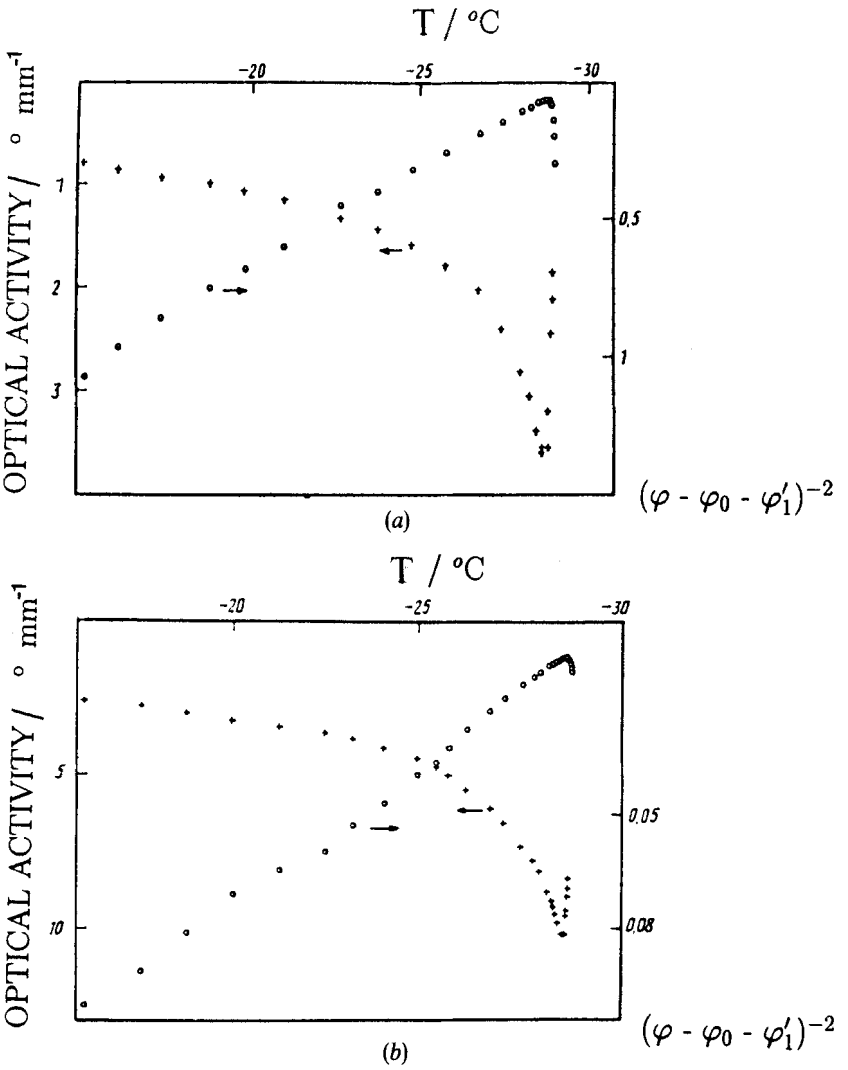

Figure 7. Optical activity in the isotropic liquid of CB15 at wavelengths of He–Ne (*a*) and He–Cd (*b*) lasers (+), and the temperature dependence of $(\psi-\psi_0-\psi_1')^{-2}$, (○) from [8].

The Landau–de Gennes free energy can be written as

$$F = F_0 + F_2(\varepsilon) + F_3(\varepsilon) + F_4(\varepsilon), \tag{2}$$

with

$$F_2 = \frac{1}{2}\int dr\left[aSp(\varepsilon^2) + b\left(\frac{\partial \varepsilon_{ij}}{\partial x_k}\right)^2 + c\left(\frac{\partial \varepsilon_{ij}}{\partial x_i}\right)^2 + 2bdqe_{ijk}\varepsilon_{il}\frac{\partial \varepsilon_{ij}}{\partial x_k}\right], \tag{3}$$

$$F_3 = \beta\int dr Sp(\varepsilon^3), \tag{4}$$

$$F_4 = \lambda\int dr[Sp(\varepsilon^2)]^2, \tag{5}$$

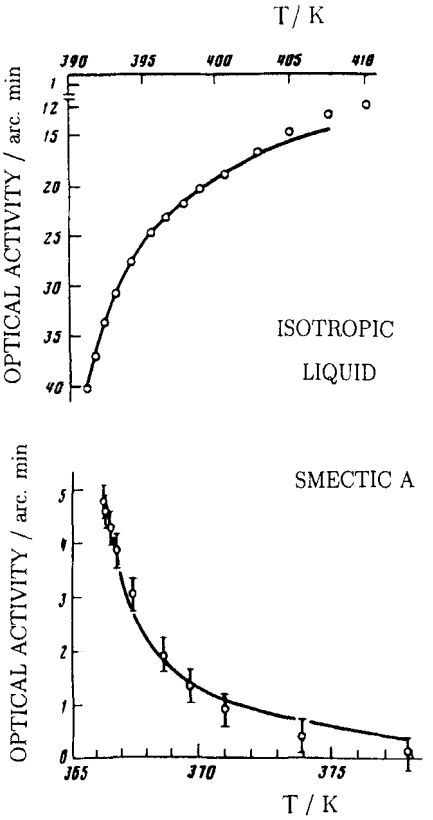

Figure 8. Pretransitional optical activity in the isotropic liquid of the ferroelectric compound DOBAMBC ($\lambda = 633$ nm, $d = 1$ mm) and in the smectic A phase with a director orientation parallel to the light beam ($\lambda = 442$ nm, $d = 0{\cdot}1$ mm) from [6].

where a, b, c, β, λ are expansion coefficients, $a_0 = a_0(T - T^*)$, δ_{ij} is the Kronecker symbol and q is the wave vector of the helical structure. The order parameter ε_{ij} is Fourier developed and then the tensorial coefficients are expanded in terms of irreducible representations of the group of rotations around the structural wave vector τ (Brazovskij *et al.* [10–11]; Hornreich and Shtrikman [16]; Belyakov and Dmitrienko [12])

$$\varepsilon(\mathbf{r}) = \sum_{\tau} \varepsilon^{\tau} \exp(i\tau\mathbf{r}), \tag{6}$$

$$\varepsilon^{\tau} = \sum_{m=-2}^{m=2} \varepsilon(\tau, m)\sigma_m, \tag{7}$$

where σ_m are basic matrices.

The structural modes $m = 0, \pm 1, \pm 2$ describe the long range order in the blue phases and the short range order of the chiral type in the isotropic liquid of chiral liquid crystals. Modes $m = \pm 1$ are called conic spiral modes and $m = \pm 2$ are plane spiral modes. The sign of the mode corresponds to the sign of the helix in the cholesteric phase. The local structure of the plane spiral mode corresponds to the common plane cholesteric spiral (see figure 9). The $m = 1$ mode describes a conic spiral with an angle of 45° between the helix axis and the director. The quasi-nematic mode $m = 0$ gives no

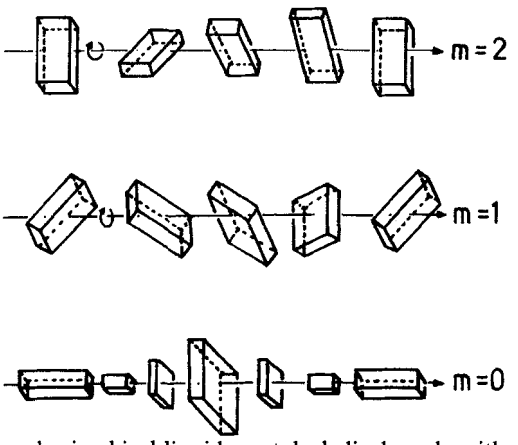

Figure 9. Structural modes in chiral liquid crystals: helical mode with plane spiral structure ($m=2$), conical spiral structure ($m=1$) and quasi-nematic mode (from [46]).

contribution to the optical rotation and is important for the interpretation of light scattering data, therefore we shall discuss further only the chiral structural modes $m=1,2$.

In the isotropic liquid, the correlation lengths of the structural modes have different temperature dependences

$$\xi_1=\left[\frac{b(1+c/2b)}{a_0(T-T_1^*)}\right]^{1/2}, \tag{8}$$

$$\xi_2=\left[\frac{b}{a_0(T-T_2^*)}\right]^{1/2}, \tag{9}$$

where T_1^*, T_2^* are temperatures of absolute instability of these conic and plane spiral modes

$$T_1^*=T^*+\frac{bq^2}{4a_0(1+c/2b)}, \tag{10}$$

$$T_2^*=T^*+\frac{bq^2}{a_0}, \tag{11}$$

where T^* is temperature of absolute instability of the isotropic liquid. It can be seen that $T_1^*\leqslant T_2^*$. The difference between T_1^* and T_2^* is the difference in the energy spectra of these excitations and the energetical preference of the $m=2$ mode. These differences are the fundamental reasons for the observed anomalies in pretransitional effects.

Measurements of the optical rotation in the isotropic liquids of chiral liquid crystals make it possible to determine the correlation lengths and temperatures T_1^* and the T_2^* [8]. In accordance with theoretical and experimental investigations, the rotation of the polarization plane of light in the isotropic liquie of chiral liquid crystals can be expressed as a sum of four terms

$$\psi=\psi_0+\psi_1+\psi_1'+\psi_2, \tag{12}$$

where ψ_0 is the intrinsic molecular rotation of the plane of polarization of light, ψ_1 is the rotation of the polarization plane of light by fluctuations of conic mode ($m=1$), ψ_1' is a term, taking into account the cut-off in continuum theory at molecular distances and

ψ_2 is the rotation of the plane polarization of light by fluctuations of plane spiral mode ($m=2$).

The terms ψ_1, ψ_2, ψ'_1 can be expressed in the following form:

$$\psi_1 = \frac{k_0^2 q k_B T}{48\pi\varepsilon_0^2 b(1+c/2b)^2}\xi_1, \tag{13}$$

$$\psi'_1 = -\frac{k_0^2 q k_B T l}{12\pi^2\varepsilon_0^2 b(1+c/2b)^2}, \tag{14}$$

$$\psi_2 = -Im\left\{\frac{k_B T k_0^3}{16b\varepsilon_0^2\pi}\xi_2 F(a_1)\right\}, \tag{15}$$

where $k_0=(2\pi n)/\lambda$ is the wave vector of the light, $q=(4\pi n)/\lambda_B$ is the structural wave vector of the cholesteric phase, l_0 is a constant characterizing a range of distances where the continuous theory is not applicable at normal pressure and $\varepsilon_0=n^2$ is an average dielectric constant. The function $F(a_1)$ was calculated by Dmitrienko [8] and

$$a_1 = \frac{q+i\xi_2^{-1}}{2k_0}. \tag{16}$$

Using expressions (13)–(15), the Landau coefficients and the correlation lengths in the case of temperature pretransitional effects at constant pressure have been determined [8].

By changing the pressure in isothermal measurements, a maximum of optical rotation in the isotropic liquid of the cholesterogen CE2 (BDH) [4-(2-methylbutyl-phenyl) 4'-(2-methylbutyl)biphenyl-4-carboxylate] has be recently observed as shown in figure 10 [44, 45]. The optical activity of CE2 increases with increasing pressure in the direction towards the clearing point, runs through a maximum and then decreases. The sign of the optical rotation is not changed in the isotropic liquid. All experimental points presented in figure 10 belong to the isotropic liquid. To explain this effect, we take into account a shift of the temperatures of absolute instability of the fluctuation modes and a change of a typical intermolecular distance as a linear function of pressure. This is justified, as the effects of pressure on liquid crystals are small and, for example, the cholesteric pitch remains approximately constant in these experiments. Pressure induced shift of the temperature of absolute instability of the fluctuation modes T_m^* ($m=1,2$) can be expressed as follows:

$$T_m^*(p) = T_{m,0}^* + \beta p, \tag{17}$$

where $T_{m,0}^*$ is the temperature of absolute instability of the mth fluctuation mode at normal pressure, p is pressure and β is the expansion coefficient.

Correlation lengths can be expressed in the form

$$\xi_1 = \left[\frac{b}{a_0}\left(1+\frac{c}{2b}\right)\frac{1}{\beta(p_1^*-p)}\right]^{0.5}, \tag{18}$$

$$\xi_2 = \left[\frac{b}{a_0}\frac{1}{\beta(p_2^*-p)}\right]^{0.5}, \tag{19}$$

where a_0, b are coefficients of the Landau free energy [10, 11] and

$$p_m^* = \frac{1}{\beta}(T - T_{m,0}^*). \tag{20}$$

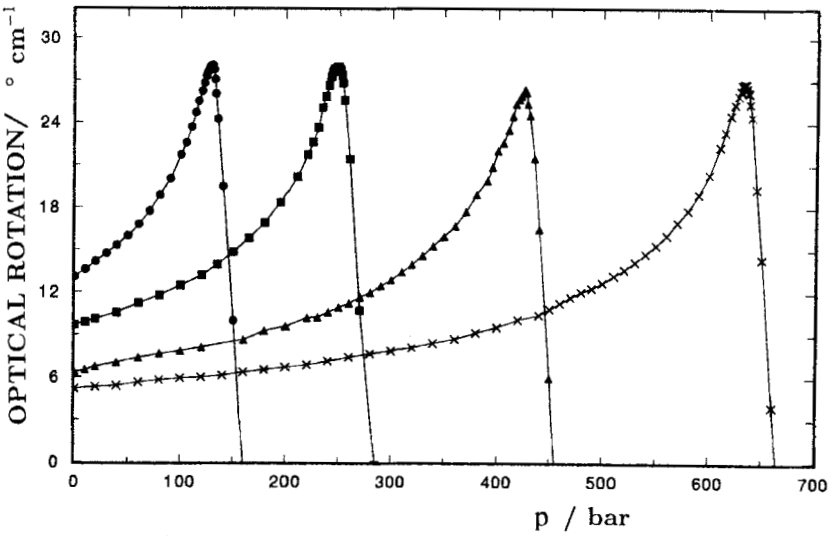

Figure 10. Pressure dependence of optical activity of CE2 for isotherms at 398 K (●), 403 K (■), 413 K (▲), 423 K (×) [45].

For the intermolecular distance l we use the following expression:

$$l(p) = l_0 + \frac{\partial l}{\partial p} p, \tag{21}$$

where $\partial l/\partial p$ is the linear compressibility of the substance. Modification of the $m=2$ contribution for the pressure induced effects proceeds by substitution of the correlation length $\xi_2(p)$ into (15). Using these substitutions we obtain

$$\psi(p) = \psi_0 + \frac{k_0^2 q k_B T}{48\pi\varepsilon_0^2[1+c/2b]^{3/2}(a_0 b)^{1/2}(\beta(p_1^* - p))^{1/2}} + \psi'_{1,0} + \gamma p + \psi_2(p), \tag{22}$$

where $\psi'_{1,0}, \gamma$ are constants, which can be simply calculated from the above expressions.

Contributions ψ_1 and ψ_2, which essentially determine the pressure dependence of the optical rotation always have opposite signs for the wavelength of measurements lying in the visible spectral interval and for values of the cholesteric pitch for cases in which the effect of the inversion of sign can be observed [5, 6–9] ($\lambda_B \leqslant 350$ nm). In [8] it has been shown that the plane spiral mode contribution is to be taken into account in the temperature interval of about 1°C above the clearing point and falls as ξ^3 far away from the phase transition temperature. Pressure dependence of the optical rotation far away from the clearing point can be described by a contribution of the conic spiral mode. Numerical modelling of equation (22) shows that the maximum in the optical rotation can be observed for short pitch cholesteric liquid crystals in the isotropic liquid in the vicinity of the clearing point. Energy spectra of structural modes in parabolic approximation, obtained in [10, 11], show an energetical preference for the $m=2$ mode. As the result of this, the correlation length ξ of the $m=2$ fluctuations diverges at smaller pressures with respect to the $m=1$ mode. Hence, anomalous growth of the correlation length of the plane spiral mode in the vicinity of the phase transition isotropic liquid–blue phase leads to the occurrence of a maximum of the optical activity in the isotropic liquid. Real inversion of the sign of optical rotation does not necessarily

take place. This depends on the relation between the wavelength of measurement and the cholesteric pitch.

To fit the experimental data of figure 9, far away from the phase transition temperature in accordance with [17–22], the following formulae have been used [45]:

$$(\psi-\psi_0-\psi'_1)^{-2}=B_0T(p_1^*-p),\ \psi'_1=-0{\cdot}016\times T+\gamma p, \tag{23}$$

where B_0, p_1^* and γ are fitting parameters.

Figure 11 shows an excellent linearity of $(\psi-\psi_0-\psi_1)^{-2}$ versus p for $T=150°C$, $B_0=70\pm5\times10^{-9}\,\mathrm{bar^{-1}\,K^{-1}\,cm^2\,deg^{-2}}$, $\gamma=10^{-3}\,\mathrm{deg\,cm\,bar^{-1}}$ in a broad interval of pressures. Deviation from the linearity in figure 11 takes place in close proximity to the clearing point and is caused by the necessity of taking into account the plane spiral mode contribution. The pressure interval, where this deviation takes place, increases with decreasing temperature of the isothermal regime. A fitting procedure has been carried out for several temperatures to obtain the dependence $p_1^*(T)$.

Figure 12 shows a part of the pressure–temperature phase diagram (p_c is clearing pressure) and the temperature dependence of p_1^*. The value of p_1^* is linear with Tover a broad temperature interval in accordance with [5]. Experimental curves $\phi(p)$ cannot be linearized by such a procedure for the isotherms in an interval $0°C\leqslant(T-T_C)\leqslant3°C$, where T_C is the clearing point under normal conditions. In this interval, the plane spiral mode contribution should be taken into account. These measurements allow the determination of the Landau expansion coefficients and the correlation length by analogy with [8].

Based on the results of [8] and [45], we can now describe some details of the phase transition isotropic liquid–BPIII. During this phase transition, the correlation length characterizing the short range order is changed. Maximal values of the fluctuation correlation length in the isotropic liquid, obtained in [8] and [45], are about 150–200 Å. The dimension of the domains in the amorphous BPIII structure is about 1 μm (depending on the chirality of the substance) [25, 32]. We can say nothing about the

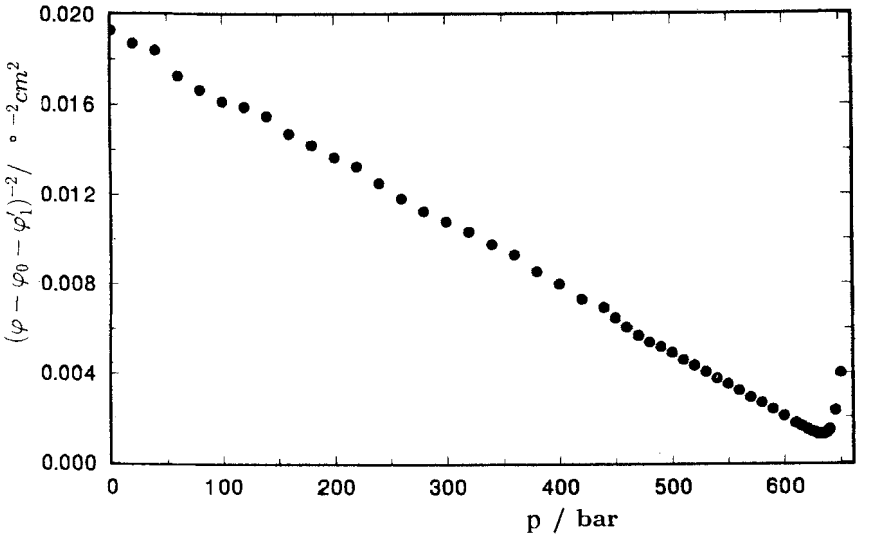

Figure 11. Pressure dependence of $(\psi-\psi_0-\psi'_1)^{-2}$ for the temperature $T=423$ K.

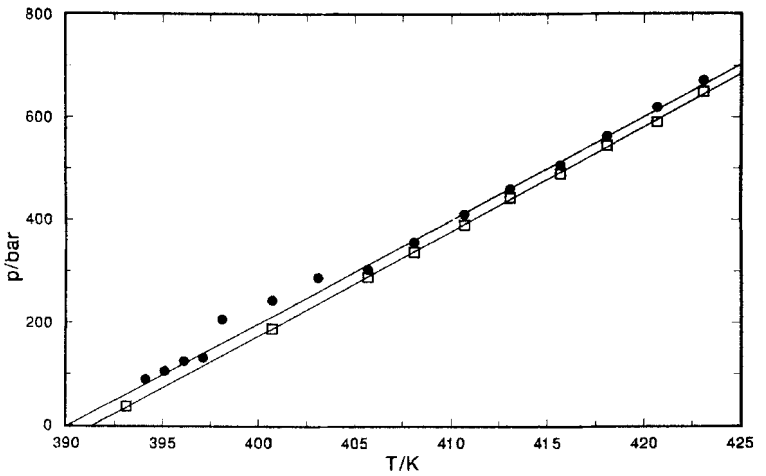

Figure 12. The temperature dependence of pressure of absolute instability of the conic mode fluctuations p_1^* (●) and clearing pressure p_c (□).

change of local symmetry during this transition as there is no information about the local symmetry of the isotropic liquid in this case.

Large pretransitional effects of the optical activity have been observed in the isotropic liquid of ferroelectric liquid crystals in [6] (see figure 8) and recently repeated in [49]. The difference $T_1^* - T_C$ is of the order of 3 K and the plane spiral mode contribution can be neglected. The theory of Filev [42] gives a successful description of the experimental data over a large temperature interval.

2.2. *Fluctuational optical activity of the smectic A phase in ferroelectric liquid crystals*

In [6], fluctuational optical rotation in the smectic A phase of the ferroelectric liquid crystal DOBAMBC was observed (see figure 8). Optical activity was measured on S_A samples with perfect monodomain texture, with the smectic planes oriented parallel to the substrate. Such a geometry enables us to measure the pure optical rotation without a birefringence contribution from the highly anisotropic smectic A phase. The important feature of the observed effect consists in a change of the sign of optical rotation in the smectic A phase with respect to the isotropic liquid. The theory of Filev [6] describes this effect as an optical rotation combined with soft mode vibrations of the director in the smectic A phase. The Landau–de Gennes free energy has the following form:

$$\frac{(F-F_0)}{T}=\frac{1}{2}\int\left\{a\beta_\alpha^2+b_c\left(\frac{\partial\beta_\gamma}{\partial x_\alpha}\right)^2+2b_c q_c e_{\alpha\beta\gamma}\beta_\gamma\frac{\partial\beta_\alpha}{\partial x_\alpha}+\lambda\beta_\alpha^2\beta_\alpha^2\right\}dr, \tag{24}$$

where $\boldsymbol{\beta}=(\beta_1,\beta_2,0)$; a, b_c, λ are expansion coefficients, $q_c=(2\pi\sqrt{\varepsilon_0})/\lambda$ is the wave vector of the conical spiral; the z coordinate is directed along the smectic plane normal. By analogy with cholesteric liquid crystals, the tensorial order parameter $\mathbf{Q}_{\alpha\beta}$ has the form

$$\mathbf{Q}_{\alpha\beta}(\mathbf{q})=\Delta\varepsilon[\beta_\alpha(\mathbf{q})n_\gamma+n_\alpha\beta_\gamma(\mathbf{q})], \tag{25}$$

where $\Delta\varepsilon$ is the anisotropy of the dielectric constant.

For the light wave vector $\mathbf{k}_0 \| \mathbf{n}$ we obtain the expression for the anisotropy of the dielectric tensor

$$\varepsilon_{\alpha\gamma}(\mathbf{k}_0) - \varepsilon_{\alpha\gamma}(\mathbf{k}_0) = -\frac{2(\Delta\varepsilon)^2 k_0 q_c \xi_A}{15\pi\varepsilon_0 b_c} L_{\alpha\gamma}, \tag{26}$$

where $\xi_A = (b_c/a)^{1/2}$ is the correlation length of fluctuations of the soft mode type in the smectic A phase, $L_{\alpha\gamma} = ie_{\alpha\gamma\mu}k_\mu/k$. An analogous expression for the conical spiral mode contribution in the isotropic liquid at the phase transition into the cholesteric (blue) phase has the form

$$\varepsilon_{\alpha\gamma}(\mathbf{k}_0) - \varepsilon_{\alpha\gamma}(\mathbf{k}_0) = \frac{k_0 q \xi_1}{6\pi\varepsilon_0 b} L_{\alpha\beta}. \tag{27}$$

An important condition in this case is $\xi_{1,A} \ll \lambda, \lambda_B$, which applies in the experiments [6].

Experimentally observed effects of fluctuation rotation of the plane of polarization of light in the isotropic liquid and the smectic A phase of several highly chiral liquid crystals was successfully described in the framework of the mean field theory. Landau coefficients a_0, b as well as the correlation lengths are estimated.

We can now describe these effects in the language common for the theory of spatial dispersion [1]. In accordance with [43], effects of spatial dispersion on the dielectric tensor ε_{ij} will be taken into account as linear and quadratic terms in the wave vector of light $\mathbf{k}$

$$\varepsilon_{ij}(\omega, \mathbf{k}) = \varepsilon_{ij}(\omega) + i\gamma_{ijl}k_l + \alpha_{ijlm}k_l k_m. \tag{28}$$

We shall use the results of equation (28) only in a quantitative way to draw an analogy between the solid state and liquid crystals. The fluctuational optical rotation in the isotropic liquid is an effect of first order in (a/λ) [43], where a in our case is the correlation length in the isotropic liquid or the smectic A phase. This conclusion is also true for the fluctuation contribution of the plane spiral mode, where the tensor γ_{ijl} is proportional to $(a/\lambda)^2$. Higher order contributions are not important in this case. But we shall further describe the experimental situation, where quadratic contributions in (a/λ) determine the main effect in optically active substances.

2.3. *Structural optical rotation in cholesteric and blue phases*

The optical activity of cholesteric and blue phases is one of their most important properties. It has been extensively investigated experimentally and theoretically and has been well known for a long time (for a review see [3]). In this part we shall discuss the optical rotation from the point of view of the determination of structural parameters of chiral phases which are an important feature of the effect of spatial dispersion. We shall concentrate our attention on the more general case of the optical activity of blue phases, which includes as a particular case the optical activity of the cholesteric phase.

The optical activity of blue phases has been investigated theoretically and experimentally in [39, 50–52]. We shall describe the order parameter of the blue phases as the anisotropic part of the dielectric tensor. To describe the optical activity in chiral liquid crystals we must take into account the change in the effective electric field in the substance during the process of the Bragg reflection of light. Thus we take the electric field vector inside the substance in the form of a Bloch wave [2, 39]

$$\mathbf{E} = \mathbf{E}_0 + \sum_{\tau \pm 0} \mathbf{E}_\tau \exp[i\mathbf{k}_\tau \mathbf{r} - i\omega t], \tag{29}$$

where $\mathbf{E}_0$ is the electric field amplitude of the incident wave; $\mathbf{E}_\tau$ is the amplitude of the diffracted wave with wave vector $\mathbf{k}_\tau$; $\tau = 4\pi n/\lambda_B$ is the structural wave vector of the blue phases. The amplitudes $\mathbf{E}_\tau$ were found in [39] by solving the Maxwell equations by perturbation theory

$$\mathbf{E}_\tau = \frac{k_0^2 \varepsilon_\tau \mathbf{E}_0 - \mathbf{k}_\tau(\mathbf{k}_\tau \varepsilon_\tau \mathbf{E}_0)}{\varepsilon_0(\mathbf{k}_\tau^2 - \mathbf{k}_0^2)}, \tag{30}$$

where $\tau \neq 0$.

In [39, 54–56] it was shown that the orientational ordering in the blue phases can be discribed to a good approximation by only taking into account the plane spiral structural mode. This means that we can express the order parameter in the following way:

$$(\varepsilon_\tau)_{ij} = \varepsilon(\tau, 2) m_{\tau i} m_{\tau j}, \tag{31}$$

where $\varepsilon(\tau, 2)$ is the amplitude of the planar mode; $\mathbf{m}_\tau = 1/\sqrt{2}(\mathbf{m}_1 - i\mathbf{m}_2)$. The vectors $\mathbf{m}_1$, $\mathbf{m}_2$, τ/τ form a real space right-hand triad. We consider further that the intrinsic polarizations of the light propagating in the substance are circular. Under these assumptions, a general expression describing the optical rotation in monodomain samples of the blue phases and the cholesteric phase per unit length was obtained [39]

$$\frac{\psi}{L} = k_0 \frac{\varepsilon_+ - \varepsilon_-}{4\varepsilon_0} = \sum_{\tau \neq 0} \frac{|\varepsilon(\tau, 2)|^2 [k_0^2 \tau^2 + (\mathbf{k}_0 \tau)^2](\mathbf{k}_0 \tau)^2}{4\varepsilon_0 \tau^3 [\tau^4 - 4(\mathbf{k}_0 \tau)^2]}, \tag{32}$$

where L is the sample thickness. Equation (32) was adapted [39] for the situations which can be realized experimentally: monodomain samples of BPI can be grown only with orientation of the wave vectors (110) or (200) perpendicular to the substrate. The monodomains of BPII can be grown with the structural wave vector (100) parallel to the sample normal. We can note now that equation (32) is equivalent to the well known de Vries formula [2] in the case of a chiral phase with a one dimensional plane spiral.

We cannot always orient our samples homogeneously. Another useful expression describes the optical rotation in polydomain samples of the blue phases. This expression, unfortunately, cannot be applied to phases possessing a macroscopic birefringence, such as the cholesteric phase, because of a strong light depolarization. In accordance with [39] we have

$$\frac{\psi}{L} = \frac{3k_0 D}{32\varepsilon_0^2} \sum_{\tau \neq 0} N_\tau |\varepsilon(\tau, 2)|^2 \int_{-1}^{1} \left(\sin x - x \cos x - \frac{x^3}{3} \right) (1 + y^2) \frac{y}{x^4} dy, \tag{33}$$

where $x = \tau D(y + \tau/2k_0)$, D is the average domain dimension and N_τ is the number of vectors given with a τ.

We shall now illustrate possibilities of this theory by two experiments: optical rotation in the monodomain and polydomain samples of cholesteryl nonanoate, and optical rotation in polydomain samples of the blue phases of the liquid crystalline polymeric material polycholesteryl acrylate (PCA-10) as described in [57].

Figure 13 shows the optical rotation in the blue phases of cholesteryl nonanoate at constant wavelength for monodomain and polydomain samples. Jumps in the experimental points correspond to phase transitions between blue phases. Equation (32) shows that optical rotation is proportional to the quadrat of the Fourier component of the order parameter $\varepsilon(\tau, 2)$. The temperature dependence of $\varepsilon(\tau, 2)$ has been determined from the optical rotation data in [39] (see figure 14). This correlates very well with values of $\varepsilon(\tau, 2)$ obtained from light reflection data for thin samples of the

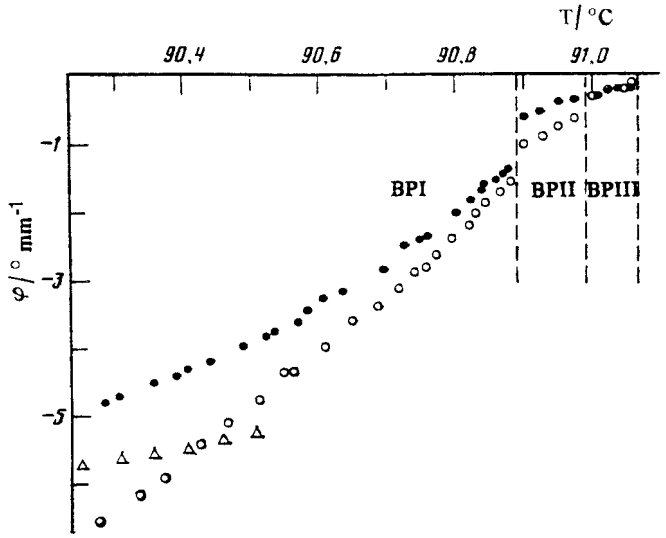

Figure 13. Optical activity of monodomain and polydomain samples of the blue phases of cholesteryl nonanoate at $\lambda = 633$ nm. (△) single crystals of the cholesteric phase, (●) BPI, BPII and BPIII polycrystals and (○) BPI, BPII and BPIII monocrystals [39].

blue phases. It is interesting to note that there is the possibility of introducing a more universal order parameter [39], which is analogous to the common nematic order parameter. This nematic order parameter (see figure 14(*b*)) shows no jumps at the transition temperatures between the blue phases [39, 56]. This means that jumps in the order parameter at transition temperatures between the blue phases and the cholesteric phase are combined only with different symmetries of these phases, and that locally blue phases are analogous to the nematic phase.

To illustrate the complicated equation (33) graphically, the authors of [39] have applied it for the description: (i) of the experiments of Collings on the optical activity of BPIII [51] (see figure 15), and (ii) of the optical rotation in polydomain samples of the blue phase of a chiral side chain polymeric material cholesteryl polyacrylate-10 (see figure 16) [57].

(i) Fitting the experimental results of Collings for the optical rotation of BPIII makes it possible to determine the structural correlation length, characterizing the short range order in the BPIII. From figure 14 it follows that the theory (33) describes the experiments quite well for $D \approx 0{\cdot}6\ \mu$m, which correlates with data obtained from reflection experiments in [25]. The discrepancy between theory and experiment at smaller wavelengths can be understood by a frequency dispersion of the refractive index in the vicinity of the absorption edge.

(ii) Blue phases in chiral polymeric liquid crystals have been observed in [58–60]. A fitting of our optical activity dispersion data enabled us to determine for the first time the amplitude of the Fourier component $\varepsilon(\tau, 2)$ and the domain dimension of the blue phase in these materials. For the blue phase in PCA-10 we obtained $\varepsilon(\tau, 2) \approx 0{\cdot}013$, and $D/\lambda_B \approx 1{\cdot}5$. Comparison of $\varepsilon(\tau, 2)$ with analogous data for the low molecular weight compound cholesteryl nonanoate (CN) (see figure 14), in which molecules have a similar chemical structure to the side groups of PCA-10, shows that, in the high molecular weight compound, the

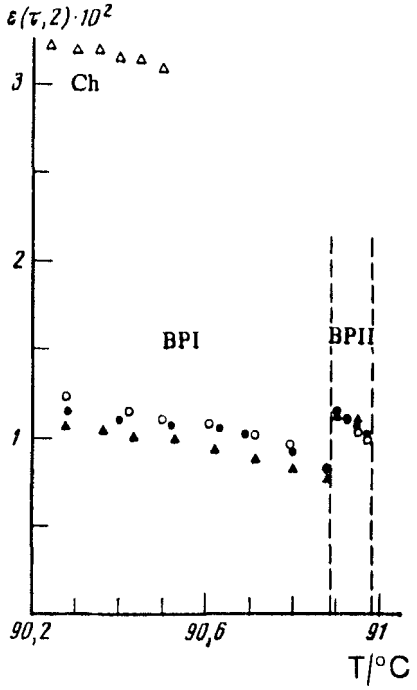

(*a*)

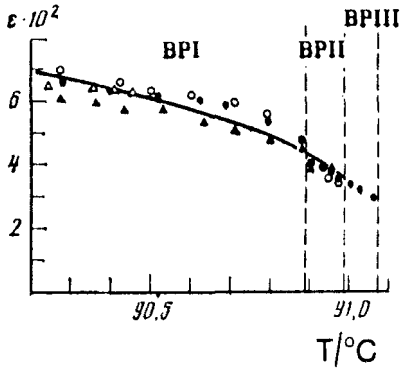

(*b*)

Figure 14. (*a*) Temperature dependence of the Fourier amplitude $\varepsilon(\tau, 2)$ from the (△) optical activity of monodomain samples of the cholesteric phase; (▲) integral intensity of the Bragg diffraction lines of BPI, BPII single crystals in transmission spectra; (○) optical activity of BPI and BPII single crystals at $\lambda = 633$ nm; (●) the same for polydomain samples of BPI and BPII; (*b*) temperature dependence of the scalar order parameter $\varepsilon(T)$ [39]. Notations of points are as those in (*a*). The order parameter of the BPIII has been calculated from the optical activity data assuming that BPIII is a polydomain texture with cubic symmetry group O^5; the icosahedral model gives approximately the same results.

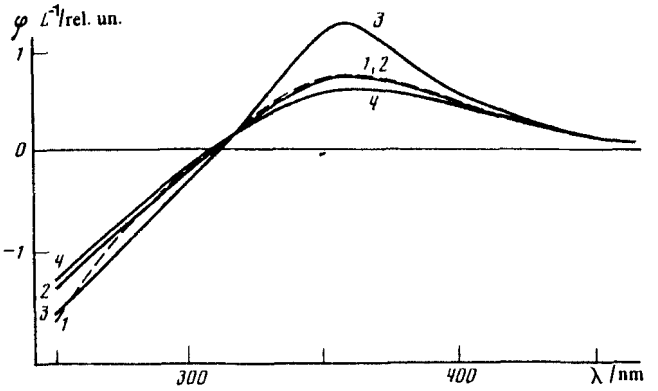

Figure 15. Experimental results of Collings [51] (1) on the optical activity in BPIII of cholesteryl nonanoate and theoretical curves calculated from (33) (2–4) with dimension of BPIII domains 0·6, 1·2, 0·5 μm respectively.

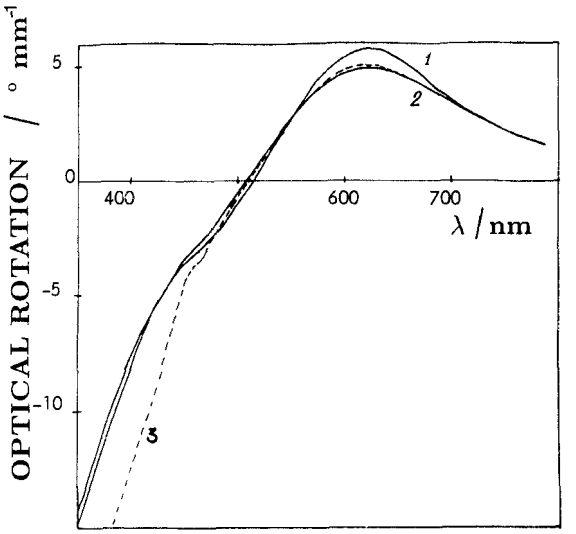

Figure 16. Theoretical ORD curves for polycrystals of the blue phase of the polymer PCA-10 with domain dimensions 1 μm (2) and the experimental curve 3.

order parameter is approximately the same as in CN [39]. The ratio of D/λ for polydomain samples in the blue phases of PCA-10 is smaller than in BPIII of CN [25, 32], which possesses the smallest domains of all blue phases [25]. This is typical for polymeric materials and is a manifestation of the influence of the main chain.

In [3, 12, 39] the effect of linear birefringence Δn of the blue phases was discussed. This effect is combined with the effects of multiple scattering of light. Serious consideration [12, 52] shows that the eigenpolarizations of light waves propagating through the substance are elliptical in the vicinity of the Bragg reflection. In other

words in the vicinity of selective reflection, a sample of a blue phase can be considered as being birefringent. The value of this birefringence was expressed in [12] as

$$\Delta n = 2\psi \frac{(\mathbf{k}_0 \mathbf{s})}{\mathbf{k}_0^2 L}, \tag{34}$$

where ψ is optical rotation of the sample, $\mathbf{s}$ is the unit vector parallel to the sample normal and, L is the sample thickness. But, from the point of view of spatial dispersion, this effect is of the same order as the optical rotation and is equal to zero if the optical activity is zero. In section 3 we shall discuss other spatial dispersion effects, which do not vanish in the case of zero rotation of the plane polarization of light. In concluding, the theory of the optical properties of cholesteric liquid crystals describes quite well the data on structural optical activity. Comparison of theory and experiment makes it possible to determine the amplitudes of the Fourier components of the order parameter. Optical rotation measurement is a very sensitive structural method in the case of blue phases: to each Fourier component of the order parameter corresponds some peculiarities in the optical rotation dispersion curves (see figure 16). Structural optical activity is also a spatial dispersion effect of the first order in (a/λ). The proportionality of optical activity to [43] (a^3/λ^4) is combined with the dependence of the tensor γ_{ijl} on the wave vector of light, see equation (28) [39, 43].

3. Spatial dispersion effects of higher orders

The investigation of spatial dispersion is a wide area of experimental and theoretical work in solid state physics (all important references can be found in [1]). In liquid crystals, however, it has been restricted to the optical activity in chiral liquid crystals. Spatial dispersion effects of higher orders in a girotropic medium are not known. In our experiments we have observed two new effects: an anomaly of the refractive index of the blue phases in the vicinity of the Bragg reflection wavelength [61, 62] and an optical anisotropy of cubic blue phases in the wavelength region of transmission by the substance. In a mirror cell used in our investigations, the contribution of the optical rotation is clearly equal to zero. Therefore, we believe that we see effects of higher orders in (a/λ) in optically active media. We shall describe in this chapter our recent experiments on blue phases and cholesterics and then discuss these phenomena on the basis of the theory developed for spatial dispersion effects in the solid state [1].

3.1. *Experimental*

The experimental set up for the investigation of electro-optic properties of chiral liquid crystals by means of interference microscopy and the construction of the mirror cell were realized for the first time by Niggemann [62]. We have measured the refractive index dispersion in cholesteric and blue phases of cholesteric–nematic mixtures with different optical anisotropy. The first class of mixtures exhibited a large optical anisotropy and consisted of 60·9 and 53·5 wt% of the highly chiral compound CB15 [4-cyano-4′-(2-methylbutyl)biphenyl] (Merck Ltd) and the wide range nematic mixture E9 (Merck Ltd). These mixtures exhibit the following phase transitions between liquid-crystalline phases of interest (in degrees centigrade):

Ch 20·21 BPI 20·66 BPII 20·86 BPIII 21·36 I (60·9 per cent CB15);
Ch 29·00 BPI 29·42 BPII 29·52 BPII + I 29·60 I (53·5 per cent CB15).

The optical anisotropy Δn was measured for the cholesteric phase at the phase transition Ch–BPI using an Abbé refractometer and was about 0·094 [62]. The

concentration dependence of this value is relatively small in this range of concentrations.

A second mixture was made of 34 mol% of the pure nematic compound CCN 55 [4,4'-di-n-pentyl-1-bicyclohexyl-4-carbonitrile] (E. Merck), which has a negative sign of the dielectric anisotropy in the kHz frequency interval, and the pure, highly chiral compound CE2. The optical anisotropy of this mixture, at the phase transition cholesteric–BP, was $\Delta n = 0{\cdot}038$ [62]. Phase diagrams of these mixtures are given in [48, 62].

To compensate for the optical rotation of the chiral phases, a mirror cell was used. The experimental cell consists of two glass plates with fibre spacers between them. The upper glass was covered with a thin transparent ITO film and the lower one was an aluminium mirror. Both glasses had been coated with polyimide and uniaxially rubbed. For our experiments, it was important to have good quality monodomain samples of the blue phases. For this purpose, we used the following procedure. An electric field was applied to the sample in the temperature interval of the blue phases of such a value that no phase transition from the blue phases to other phases was induced; it was held there for about 20 min. Then the field was slowly switched off and the orientation of the blue phase relaxed to some stable position in accordance with boundary conditions for the director field. This procedure makes it possible to fix two axes of an elementary cell of a blue phase: one along the sample normal and the second along the rubbing direction. The relaxation time for the BPII was about one hour and for the BPI 2–3 days. In the first stages of the relaxation process in BPI, we have seen the formation of the so-called cross-hatching texture, consisting of birefringent domains. This texture has been described in previous work on blue phases [13, 63, 64]. The cross-hatching texture in

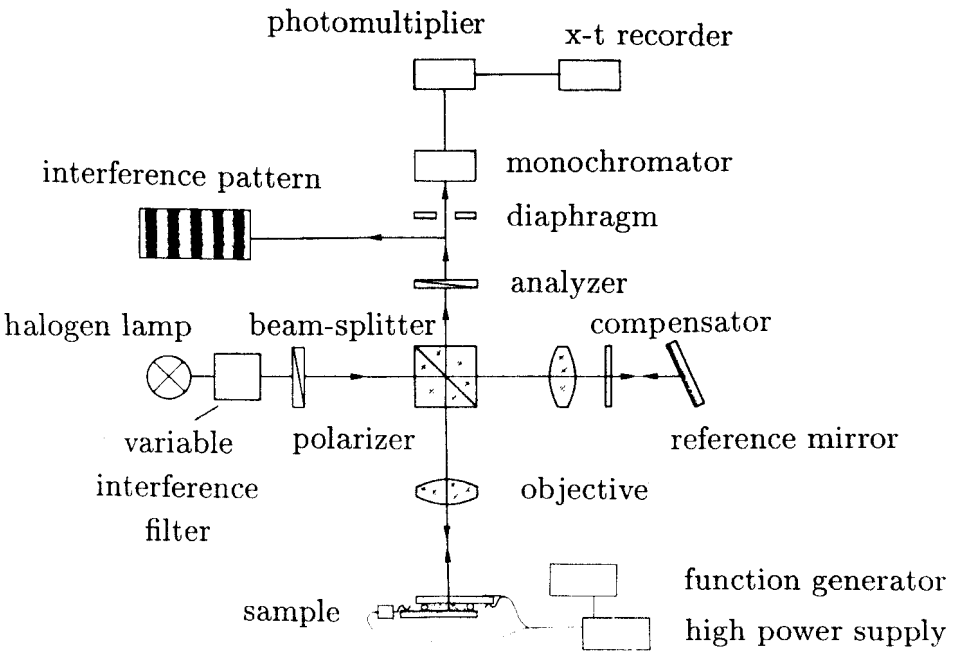

Figure 17. The experimental set up of the modified Linnik interferometer for measurements of selective reflective and refractive index dispersion.

BPI is caused by deformations occurring as a result of paramorphosis during the phase transition from BPII and relaxes to defect free samples after some time. Effects reported further in this paper have no relation to the properties of those strained samples. After the relaxation process, in our case, we obtained perfect samples of BPI without visually observable defects more than 200 μm in diameter. The structural wave vector (110) of the BPI unit cell and the wave vector (100) of the BPII are oriented by this method perpendicularly to the substrate. In the case of BPI, the wave vector ($1\bar{1}0$) was oriented along the rubbing direction and (001) oriented perpendicularly to it in the plane of substrate. The sample thickness was varied between 7 and 30 μm. We have also used ITO coated glasses without rubbed polyimide film. In this case, we have oriented only the vertical axis of the elementary cell by the field. That was (110) for BPI and (100) for BPII.

Measurements of the refractive index dispersion have been carried out with a Leitz–Orthoplan microscope equipped with a Leitz interference reflection illuminator which realizes the Linnik interference scheme, and a Jarrel Ash monochromator. Figure 17 shows the scheme of the experimental set up [61, 62]. In the microscope interferometer, the polarized or non-polarized light beam from a halogen lamp is divided by a beam splitter into two coherent beams: a reference and a testing beam. The testing beam is directed perpendicularly to the upper glass surface and, after transmission through the substance, it is reflected at the lower plate and interferes with the reference beam, which is reflected from the reference mirror. The interference pattern is detected photographically or visually in the microscope. By this method, there is no strong contribution to the optical path difference caused by the optical activity of the BPs [65]. The absolute refractive index n of a substance is determined by the simple formula [66]

$$n=\frac{m\lambda}{2d}$$

where m is the relative shift of interference stripes in the substance, with respect to an empty cell, in units of the distance between neighbouring stripes, λ is the wavelength of the light, determined by the position of the variable interference filter and d is the sample thickness. In our case, we have measured the difference between the refractive indices of a liquid crystal and a reference substance with known refractive index (cell glue Nordland UV Sealant, $n=1{\cdot}50$). The stripes shift has been measured to within one stripe, which gives an accuracy $\pm 0{\cdot}007$ in the determination of the refractive index. The dispersion change in the refractive index of the glue was smaller than the accuracy of the measurements. The measurements of the refractive index were carried out on BP monodomain samples with monochromatic light obtained by means of a variable interference filter with line width of 10 nm at the smallest diaphragms in the collimating beam. The temperature of the samples was controlled to 0·002 K.

3.2. *Results*

In the description of our experimental results we would like to consider two situations important for understanding some interesting properties of blue phases.

Figure 18 shows the dependence of the refractive index of the mixture with 60·9 per cent of CB15 in E9 on the relative wavelength in the BPI for two sample thicknesses 30 μm (*a*) and 16 μm (*b*). We have oriented BPI with the aid of an electric field. This means that samples were not oriented azimuthally. The refractive index of the isotropic liquid increases with decreasing wavelength because of the frequence dispersion in the vicinity of the absorption edge ($\lambda \approx 340$ nm). An anomaly in the refractive index of BPI

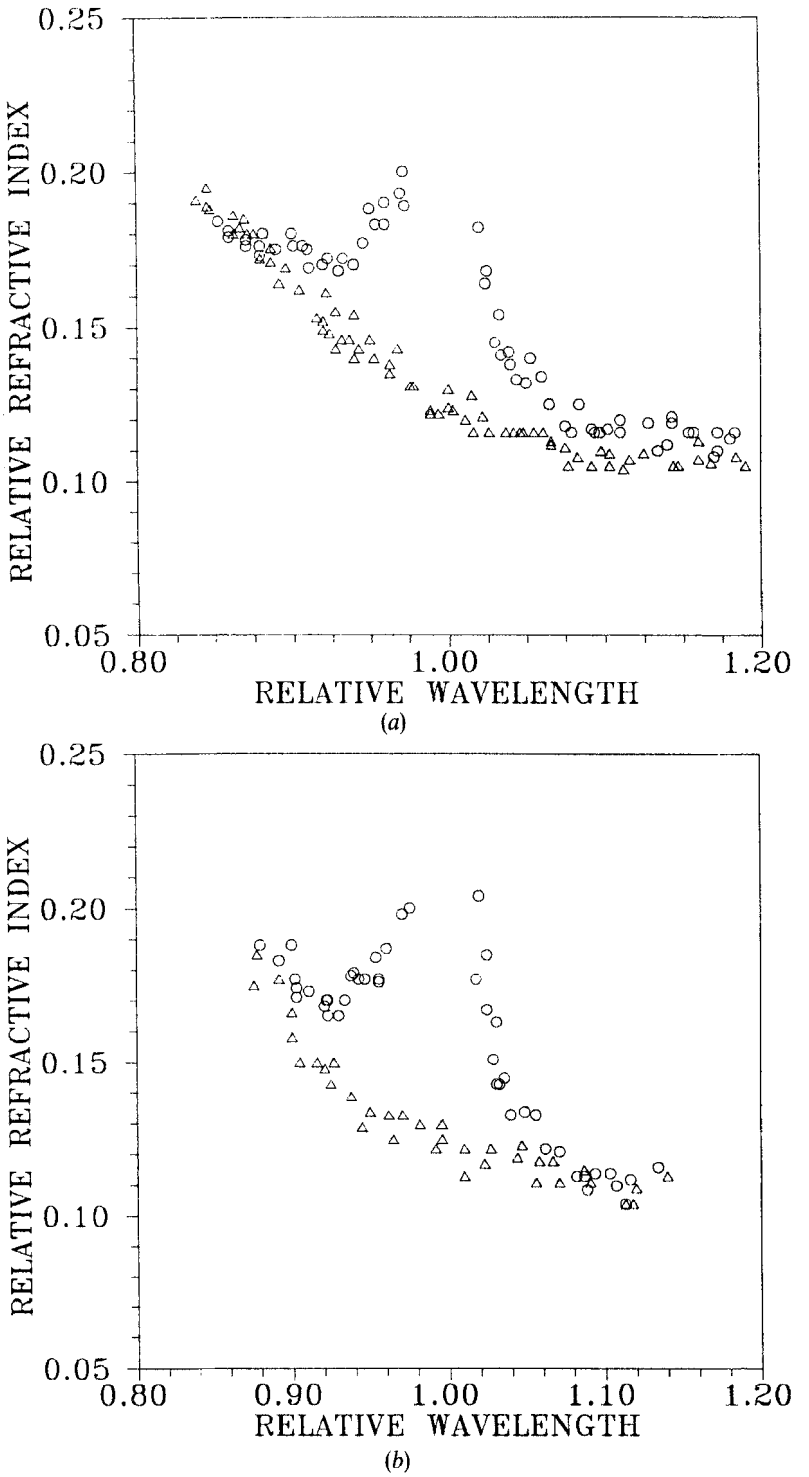

Figure 18. Relative refractive index of BPI (○) and the isotropic liquid (△) with respect to the refractive index of the reference substance versus relative wavelength λ/λ_B for a liquid crystal mixture CB15/E9 with 60·9 wt% CB15. Sample thickness: (*a*) 30 μm and (*b*) 16 μm.

in the transmission region of the mixture in the vicinity of the Bragg wavelength of BPI is observed. Refractive index dispersion in BPI in the interval of the measurements is a combination of frequency dispersion, analogous to that for the isotropic liquid and a new anomaly located at $\lambda = \lambda_B$. The refractive index increases from both sides of the selective reflection wavelength $|1 - \lambda/\lambda_B| \geqslant 0{\cdot}02$ with $\lambda_B = 541$ nm. Measurements of the refractive index were impossible in the small vicinity of λ_B, which will be clarified further by the results obtained on defect free samples of BPI. The observed effect does not depend on the sample thickness. No dependence of the refractive index on the direction of linear polarization in the plane perpendicular to the direction (110) has been observed.

Figure 19 shows the dependence of the relative refractive index of BPI in the mixture of figure 18, on the wavelength, for two directions of a linear polarization in a plane perpendicular to the (110): [001] and [1$\bar{1}$0]. Orientation of the BPI samples was azimuthally and tangentially homogeneous. The sample thickness was 30 μm. We have observed a qualitative difference between the dispersion curves for these two directions. The (1$\bar{1}$0) refractive index increases in the vicinity of λ_B, runs through a maximum and then decreases in the region of $\lambda/\lambda_B \leqslant 1$. The (001) refractive index monotonously increases on increasing the wavelength for $\lambda \leqslant \lambda_B$. For $\lambda \geqslant \lambda_B$ the refractive index in both cases decreases with increasing wavelength. For $\lambda \leqslant \lambda_B$, an anisotropy of the cubic BPI with a positive sign of $\Delta n = n_{001} - n_{1\bar{1}0}$ has been observed. The value of the anisotropy of the refractive index increases with increasing wavelength for $\lambda \leqslant \lambda_B$ and reaches

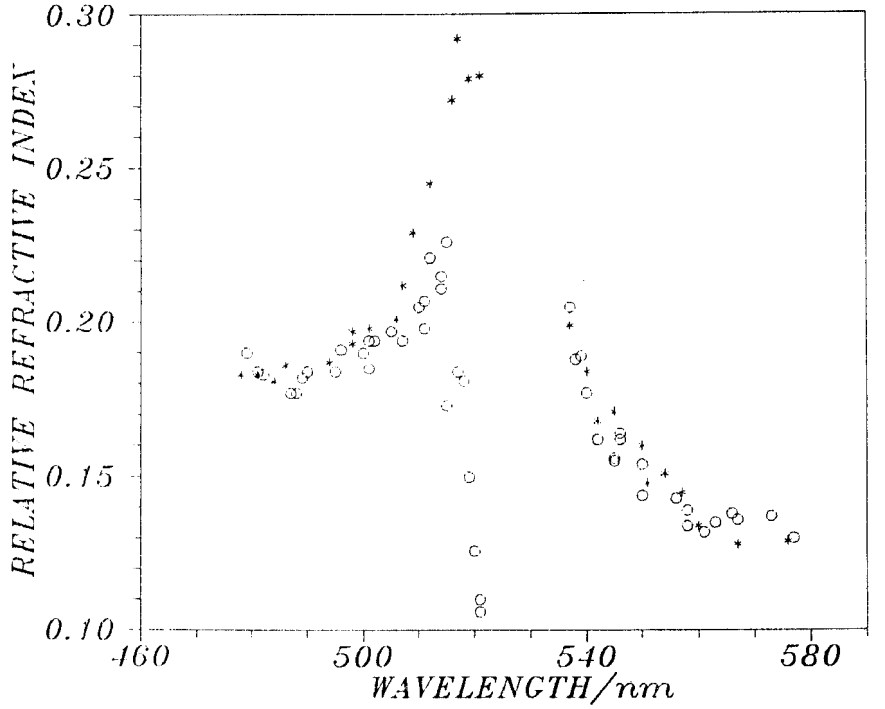

Figure 19. The refractive index dispersion curves of the BPI in a mixture with 60·9 per cent CB15 in E9 for two directions of linear polarization of the light beam propagating along the (110) direction. (○) The polarizer parallel to the direction of rubbing and (*) perpendicular to the rubbing direction.

values of the order of 0·1 in the vicinity of the Bragg wavelength. Measurements with other orientations of the polarizer in this plane show that the maximal difference between the refractive indices is found for the (001) and (1$\bar{1}$0) directions. For $\lambda \geqslant \lambda_B$ the difference between n_{001} and $n_{1\bar{1}0}$ is not larger than the accuracy of our measurements. Additionally, no sample thickness dependence was observed in this case. Figure 19 illustrates why the refractive index cannot be measured close to the Bragg reflection wavelength in the samples without homogeneous orientation of the azimuthal axes. As follows from the experimental section, we have to find the position of the zeroth stripe in the microscope field. This is impossible when domains have such strongly different refractive indices. In the case of BPII we can measure the refractive index dispersion close to λ_B without great difficulty.

Figure 20 shows the change in the refractive index dispersion curves induced by an electric field of small field strength (1 V μm^{-1}), at which no change in the texture of the BPI sample took place. The measurements were carried out on the same samples as in figure 19. The type of dependence of the refractive index on the wavelength is analogous to that of figure 19. The birefringence, Δn, of BPI decreases with increasing field, so that the anisotropy of the BPI sample can be compensated for, this value depending on the wavelength. This result verifies the theoretical prediction [67] that field induced differences in the Δn_{001} and $\Delta n_{1\bar{1}0}$ are negative and that the absolute value of the first quantity is larger than that of the second. This figure presents simultaneously the first measurement of the field induced anisotropy of BPI. For this field strength, the structural birefringence, as presented in figure 19, is equal to the field induced birefringence for wavelengths smaller than 510 nm. At higher fields, perfect monodomain samples were deformed and defects induced. We can say therefore, that, at

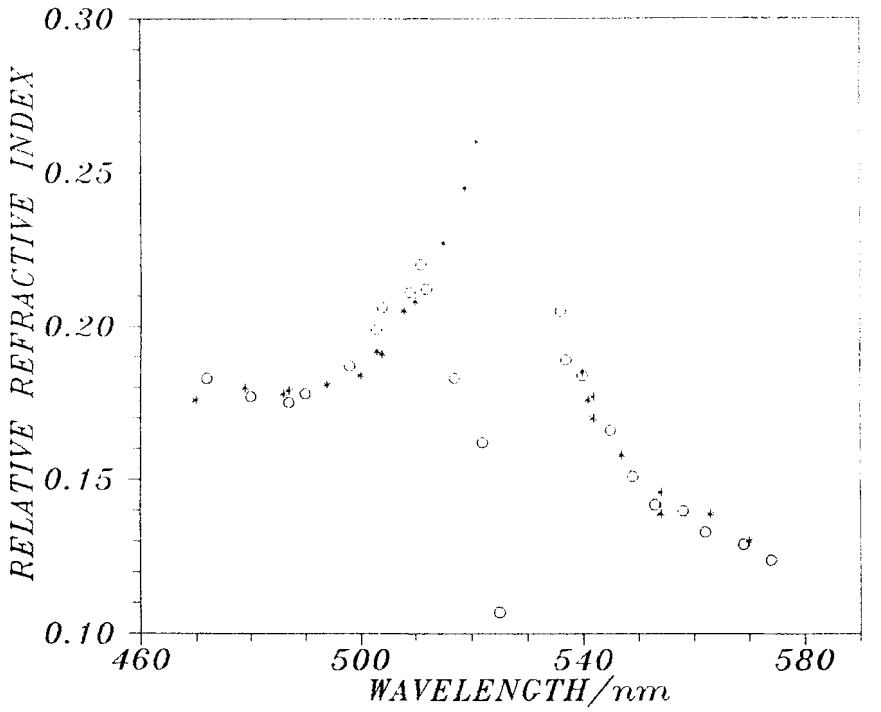

Figure 20. The field induced change of the dispersion curves in the BPI for the mixture containing 60·9 per cent CB15 in E9.

higher fields, deformations of the BPI are plastic. In other words, defects are created, and after this deformation, the sample cannot be transformed to the initial state by switching off the electric field. The change of BPI texture is reversible only after some relatively long relaxation time. In this case, deformation birefringence can play a sufficient role. Therefore, we have not measured the refractive index at fields higher than the threshold for elastic deformation.

Figure 21 presents the dependence of the refractive index on the wavelength in the BPII for a mixture with 53·5 per cent CB15 in E9 for two linear polarizations of the light beam in a plane perpendicular to (100). The samples exhibit no visible defects and were tangentially and azimuthally homogeneous. The sample thickness was 18 μm. The Bragg reflection wavelength was $\lambda_B = 557$ nm. Within the accuracy of our measurements, we see no birefringence of the BPII samples. Measurements of the dependence of the refractive index dispersion curves on the azimuthal angle in the plane perpendicular to the (100) have similary shown no change in these curves. The refractive index dependence in this case is qualitively analogous to the curves with the light wave vector $\mathbf{k}_0 \| (110)$ and polarization in the direction (001) in the case of BPI. The refractive index decreases with increasing wavelength, running through a maximum near $\lambda = \lambda_B$ and then decreases to values approximately equal to the refractive index of the isotropic liquid at $\lambda \approx 580$ nm.

Figure 22 shows the refractive index dispersion curves of the BPIII in a mixture with 59·5 per cent of CB15 in E9 in cells with strong boundary conditions. The refractive index was measured for two directions of polarization; along and perpendicular to the direction of rubbing. The maximum of the selective reflection was

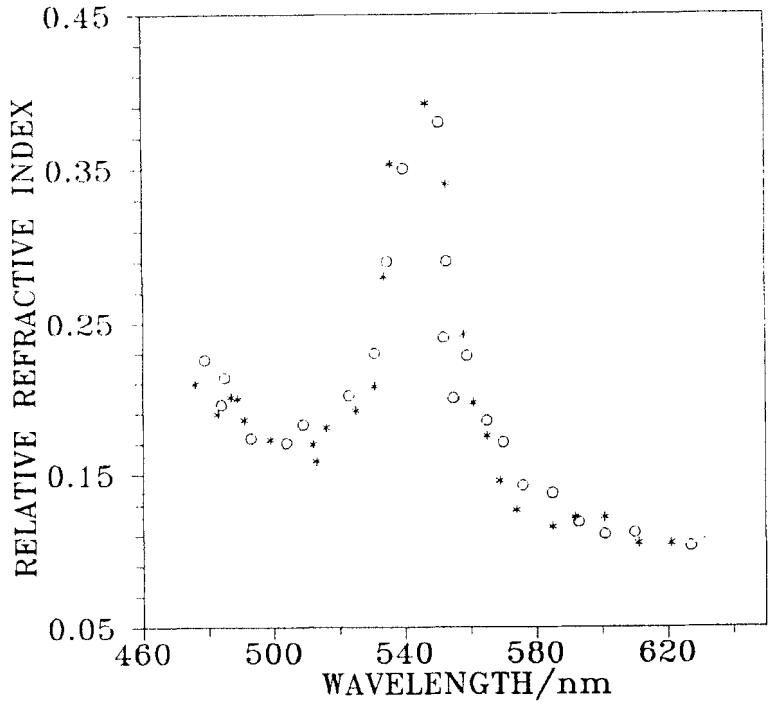

Figure 21. The refractive index dispersion curves of the BPII in a mixture with 53·5 per cent CB15 in E9 for two directions of the linear polarizer; the light beam propagating along the (100) direction. (○) Polarizer parallel to the direction of rubbing and (*) perpendicular to the rubbing direction.

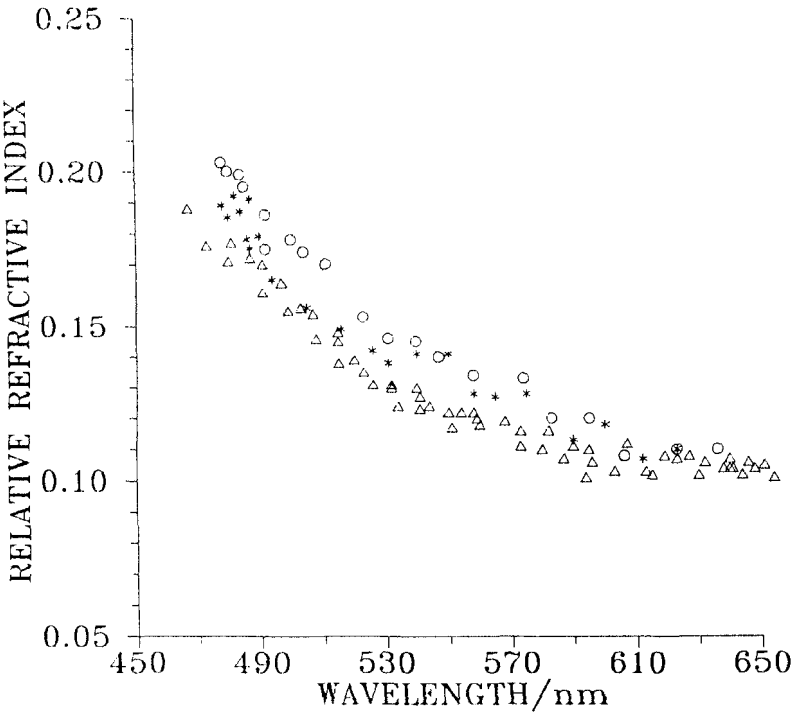

Figure 22. The refractive index dispersion curves of the BPIII in a mixture with 59·5 per cent CB15 for two directions of the linear polarizer: (○) the polarizer parallel to the direction of rubbing, (*) perpendicular to the rubbing direction and (△) isotropic liquid.

approximately at $\lambda_B = 460$ nm. The refractive index in BPIII differs from that of the isotropic liquid. This difference increases with decreasing wavelength in the direction of the selective reflection wavelength. No birefringence of BPIII was found within the accuracy of our measurements.

Figure 23 shows the refractive index dispersion for the cholesteric phase of a mixture with 49·5 per cent of CB15 in E9 in the vicinity of the Bragg reflection wavelength $\lambda_B = 530$ nm. The cholesteric samples have been oriented during the capillary flow of the substance into the cell. The sample thickness was 30 μm. At longer wavelengths, we see a difference between the refractive indices of the isotropic liquid and the cholesteric phase, which is approximately equal to 0·05 at 580 nm. The refractive index of the cholesteric phase increases faster with decreasing wavelength than that of the isotropic liquid and reaches its maximum value in the vicinity of the Bragg reflection wavelength.

Measurements of the refractive index dispersion in the blue phases of mixtures of CCN55 and CE2 have shown no peculiarity in the vicinity of the Bragg wavelength, within the accuracy of our measurements. This fact can be explained by a marked decrease in the local optical anisotropy in this type of mixture, as compared with mixture CB15/E9.

3.3. *Discussion*

In 1971, in two pieces of experimental work [68, 69], the observation of a non-trivial effect on the optical anisotropy of non-girotropic cubic crystals of silicon (Si) and gallium arsenide (GaAs) with low dislocation density was reported. This effect was

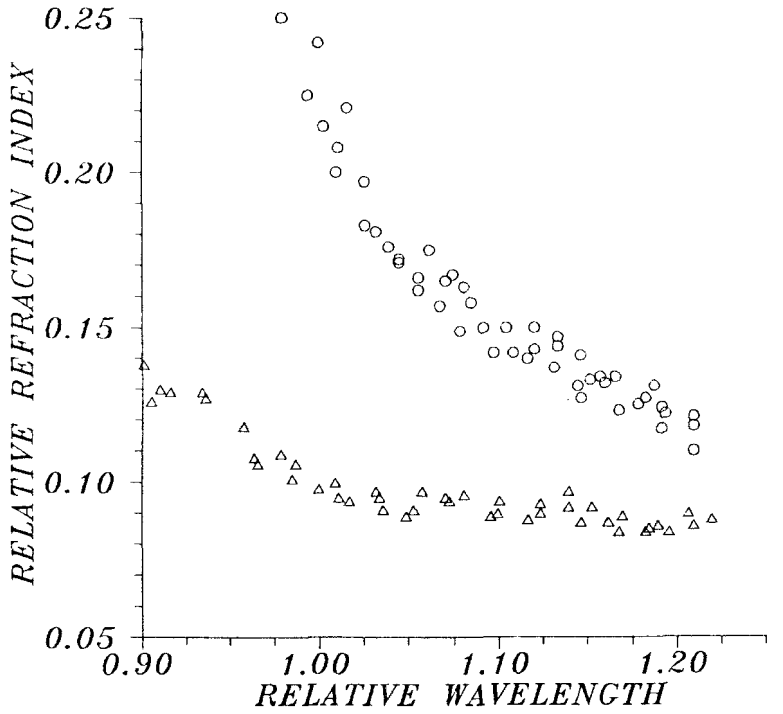

Figure 23. The refractive index anomaly in the cholesteric (○) and isotropic (△) phases of a CB15/E9 mixture containing 49·5 per cent CB15.

theoretically considered in [1, 70–73] as spatial dispersion of higher orders in (a/λ). An investigation of the effects of higher order has not been carried out experimentally up to now for girotropic materials because of the larger effect of the first order optical activity.

Effects of spatial dispersion in chiral liquid crystals have been considered theoretically [3, 12, 43, 51, 52, 74, 75]. In these theoretical studies, spatial dispersion effects of higher orders in chiral phases have not been discussed. Therefore, we shall try to understand the main features of our results in terms of the theory of spatial dispersion of higher orders in non-girotropic solid crystals developed by Ginsburg and Agranovich [1].

Firstly, let us summarize our experimental results

(1) an anomaly of the refractive index in the blue and cholesteric phases in the vicinity of the Bragg reflection wavelength is observed;
(2) defect free BPI samples are optically anisotropic in the case of propagation of light along the direction (110);
(3) defect free BPII samples are optically isotropic for light propagating along the direction (100).

It is more convenient to describe the spatial dispersion using a reciprocal tensor of the dielectric constants ε_{ij}^{-1}

$$(\mathbf{E}(\omega, \mathbf{k}) = \hat{\varepsilon}^{-1}(\omega, \mathbf{k})\mathbf{d}(\omega, \mathbf{k})). \tag{35}$$

In our case first order spatial dispersion effects are equal to zero and we take into account second order terms in the development of the reciprocal dielectric constant in powers of (a/λ). By analogy with (28) we take

$$\varepsilon_{ij}^{-1} = \delta_{ij}\varepsilon_0^{-1}(\omega) + \beta_{ijlm}k_l k_m. \tag{36}$$

To find spatial dispersion corrections of the dielectric constant we must solve the Maxwell equations. It is convenient to rewrite these equations in a form taking into account the propagation of monochromatic waves through the media

$$\mathbf{D} = -\mathbf{n}(\mathbf{s} \times \mathbf{B}), \tag{37}$$

$$\mathbf{sD} = 0, \tag{38}$$

$$\mathbf{B} = n(\omega, \mathbf{s})(\mathbf{s} \times \mathbf{B}), \tag{39}$$

$$\mathbf{D} = n^2(\omega, \mathbf{s})[\mathbf{E} - \mathbf{s}(\mathbf{sE})], \tag{40}$$

where $\mathbf{s}$ is a unit vector along the direction of the wave vector $\mathbf{k}$ of the light beam; $\mathbf{B}$ is the vector of magnetic induction; $\mathbf{D}$ is the vector of electric induction.

For the crystallographic class O (BPI and BPII), the fourth rank tensor β_{ijlm} can be simplified. In accordance with [73], in this class, the tensor β_{ijlm} possesses only three independent components β_1, β_2, β_3

$$\beta_{iiii} = \beta_1, \quad \beta_{iijj} = \beta_2, \quad \beta_{ijij} = \beta_3. \tag{41}$$

Other components are equal to zero.

Substituting equation (35) and (36) into equations (37)–(40) in [1] a system of three equations for the determination of the vector components D_j for $j = 1, 2, 3$ has been obtained

$$\frac{1}{n^2} D_j = \left(\frac{1}{\varepsilon_0} + \beta_2 n^2\right) D_j - s_j s_i D_i \left(\frac{1}{\varepsilon_0} + \beta_2 n^2\right) + \beta n^2 s_j^2 D_j - \beta n^2 s_j D_i s_i^3, \tag{43}$$

where $\beta = \beta_1 - \beta_2 - 2\beta_3$. Let us now analyse special cases which can be realized by experiment for the blue phases.

(*a*) Wave vector $\mathbf{k}$ of the light beam parallel to the edges of the elementary cubic cell ($\mathbf{k} \| (001)$). The system of equations (37)–(40) can be simplified

$$\frac{1}{n^2} D_j = \left(\frac{1}{\varepsilon_0} + \beta_2 n^2\right) D_j, \tag{44}$$

where $j = 1, 2$ and $D_3 = 0$. From (43) it follows that the refractive index of a phase with cubic symmetry does not depend on the direction of $\mathbf{D}$.

(*b*) Light wave vector parallel to the face diagonal (110) ($\mathbf{k} \| (001)$). For linear polarization along (001)

$$\frac{1}{n^2} = \frac{1}{\varepsilon_0} + \beta_2 n^2, \tag{45}$$

and for polarization along $(1\bar{1}0)$

$$\frac{1}{n^2} = \frac{1}{\varepsilon_0} + (\beta_2 + \tfrac{1}{2}\beta) n^2. \tag{46}$$

In this case, the refractive index of a cubic phase depends on the polarization of the light beam. Optical birefringence in the plane perpendicular to the direction (110) can be expressed as follows:

$$\Delta n = n_{1\bar{1}0} - n_{001} = \tfrac{1}{2}[\beta_3 + \tfrac{1}{2}(\beta_2 - \beta_1)] n^5 \frac{4\pi^2}{\lambda^2}. \tag{47}$$

For the birefringence of the non-gyrotropic solid crystal silicon, investigated in [64] the value obtained was $\Delta n \approx 5 \times 10^{-5}$. This is approximately four orders of magnitude smaller than the effect observed in our work on BPI.

The measured anisotropy of the blue phases depends on the symmetry of the direction of the propagation of light. For BPI, it can be realized experimentally that the wave vector of the light is parallel to the face diagonal of the cubic cell (rotation axis of second order). An analogous effect should also be observable for BPII in the case where we could obtain an orientation of the structural wave vector (110) perpendicular to the substrate.

This consideration of spatial dispersion effects, based on the theory developed for solid crystals can be regarded only as a first illustrative step. The other possibility to describe these effects is to take into account $m = 1$ components of the order parameter in equation (30). This possibility had not been investigated until now and deserves further attention.

The authors are grateful to Dr E. Dmitrienko and Professor E. Kats for interesting discussions and useful remarks, to Dr H. Baur (Freiburg) for production of the glasses for the experimental cells and to Dr E. Niggemann and Dr J. Hollmann for experimental measurements. This work has been supported by Alexander von Humboldt Stiftung (FRG) and the Deutsche Forschungsgemeinschaft.

References

[1] AGRANOVICH, V. M., and GINSBURG, V. L., 1984, *Crystal Optics with Spatial Dispersion, and Exitons* (Springer-Verlag), Chap. 1, p. 4.
[2] CHANDRASEKHAR, S., 1987, *Liquid Crystals* (Cambridge University Press), Chap. 4.
[3] BELYAKOV, V., and DMITRIENKO, V., 1989, *Sov. Sci. Rev.* A, *Phys.*, **13**, 1.
[4] CHENG, J., and MEYER, R., 1974, *Phys. Rev.* A, **9**, 2744.
[5] DEMIKHOV, E., and DOLGANOV, V., 1983, *JETP Lett.*, **38**, 445.
[6] DEMIKHOV, E., DOLGANOV, V., and FILEV, V., 1983, *JETP Lett.*, **37**, 361.
[7] BATTLE, P., MILLER, J., and COLLINGS, P., 1987, *Phys. Rev.*, A, **36**, 369.
[8] DEMIKHOV, E. I., and DOLGANOV, V. K., 1989, *Sov. Phys. Crystallogr.*, **34**, 723.
[9] VANWEERT, F., DEMOL, W., and VAN DAEL, W., 1989, *Liq. Crystals*, **5**, 853.
[10] BRAZOVSKII, S. A., and DMITRIEV, S. G., 1975, *Sov. Phys. JETP*, **42**, 497.
[11] BRAZOVSKII, S. A., and FILEV, V. M., 1978, *Sov. Phys. JETP*, **48**, 573.
[12] BELYAKOV, V. A., and DMITRIENKO, V. E., 1985, *Sov. Phys. Usp.*, **28**, 535.
[13] STEGEMEYER, H., BLÜMEL, T., HILTROP, K., ONUSSEIT, H., and PORSCH, F., 1986, *Liq. Crystals*, **1**, 3.
[14] CROOKER, P. P., 1989, *Liq. Crystals*, **5**, 751.
[15] WRIGHT, D. C., and MERMIN, N. D., 1989, *Rev. mod. Phys.*, **61**, 385.
[16] HORNREICH, R. M., and SHTRICKMAN, S., 1988, *Molec. Crystals liq. Crystals*, **165**, 183.
[17] BLÜMEL, T., COLLINGS, P. J., ONUSSEIT, H., and STEGEMEYER, H., 1985, *Chem. Phys. Lett.*, **116**, 529.
[18] BLÜMEL, T., ONUSSEIT, H., and STEGEMEYER, H., 1983, *Proceedings of the 13th Freiburger Arbeitstagung Flüssigkristalle, 22–25 March.*
[19] BLÜMEL, T., and STEGEMEYER, H., 1984, *J. Crystal Growth*, **66**, 163.
[20] CLADIS, P. P., PIERANSKI, and JOANIKOT, M., 1984, *Phys. Rev. Lett.*, **52**, 542.
[21] BARBET-MASSIN, R., CLADIS, P. E., and PIERANSKI, P., 1984, *Phys. Rev.* A, **30**, 1161.
[22] JOHNSON, D. L., FLACK, J. H., and CROOKER, P. P., 1980, *Phys. Rev. Lett.*, **45**, 641.
[23] MEIBOOM, S., and SAMMON, M., 1980, *Phys. Rev. Lett.*, **44**, 882.
[24] KIZEL, V. A., and PROKHOROV, V. V., 1984, *Sov. Phys. JETP*, **60**, 257.
[25] DEMIKHOV, E., DOLGANOV, V., and KRYLOVA, S. P., 1985, *JETP Lett.*, **42**, 16.
[26] CLADIS, P. E., GAREL, T., and PIERANSKI, P., 1986, *Phys. Rev. Lett.*, **57**, 2841.
[27] JEROME, B., PIERANSKI, P., GODEK, V., HARAN, G., and GERMAIN, C., 1988, *J. Phys., Paris*, **49**, 837.

[28] JEROME B., and PIERANSKI, P., 1989, *Liq. Crystals*, **5**, 799.
[29] MEIBOOM, S., SETHNA, J. P., ANDERSON, P. W., and BRINKMANN, W. F., 1981, *Phys. Rev. Lett.*, **46**, 1216.
[30] MEIBOOM, S., SAMMON, M., and BERREMAN, D., 1983, *Phys. Rev.* A, **28**, 3553.
[31] DUBOIS-VIOLETTE, E., and PANSU, B., 1988, *Molec. Crystals liq. Crystals*, **165**, 151.
[32] DEMIKHOV, E. I., DOLGANOV, V. K., and KRYLOVA, S. P., 1987, *Sov. Phys. JETP*, **66**, 998.
[33] YANG, D. K., CROOKER, P. P., and TANIMOTO, K., 1988, *Phys. Rev.* A, **37**, 4001.
[34] DEMIKHOV, E., and DOLGANOV, V., 1990, *Nuovo Cim.*, **12**, 1335.
[35] KITZEROW, H.-S., CROOKER, P. P., and HEPPKE, G., 1991, *Phys. Rev. Lett.*, **67**, 2151.
[36] FILEV, V. M., 1986, *JETP Lett.*, **43**, 677.
[37] HORNREICH, R. M., and STRICKMANN, S., 1986, *Phys. Rev. Lett.*, **56**, 1723.
[38] DEMIKHOV, E., and STEGEMEYER, H., submitted; TREBIN, H. R., FINK, W., and STARK, H., 1992, *The 18th IUPAP Conference on Statistical Physics*, Poster, Berlin, p. 218.
[39] BELYAKOV, V., DEMIKHOV, E., DMITRIENKO, V., and DOLGANOV, V., 1985, *Sov. Phys. JETP*, **62**, 1173.
[40] THOEN, J., 1988, *Phys. Rev.*, A, **37**, 1754.
[41] DOLGANOV, V. K., KRYLOVA, S. P., and FILEV, V. M., 1980, *Sov. Phys. JETP*, **57**, 1177.
[42] FILEV, V. M., 1983, *JETP Lett.*, **37**, 703.
[43] BENSIMON, D., DOMANY, E., and SHTRICKMAN, S., 1983, *Phys. Rev.* A, **28**, 427.
[44] HOLLMANN, J., and POLLMANN, P. (unpublished results).
[45] DEMIKHOV, E., HOLLMANN, J., and POLLMANN, P., 1993, *Europhysics Lett.*, **21**, 581.
[46] TREBIN, H.-R., 1988, *Phys. Bl.*, **44**, 221.
[47] MILLER, J. D., BATTLE, P. R., COLLINGS, P. J., YANG, D. K., and CROOKER, P. P., 1987, *Phys. Rev.* A, **35**, 3959.
[48] SPIER, B., 1990, Thesis, Paderborn, pp. 40–53.
[49] FRAME, F. C., WALKER, J. L., and COLLINGS, P. J., 1991, *Molec. Crystals liq. Crystals*, **198**, 91.
[50] STEGEMEYER, H., and BERGMANN, K., 1980, *Springer Series in Chemical Physics*, Vol. 11 (Springer-Verlag), p. 161.
[51] COLLINGS, P. P., 1984, *Phys. Rev.* A, **30**, 1990.
[52] BELYAKOV, V. A., DMITRIENKO, V. E., and OSADCHIJ, S. M., 1982, *Sov. Phys. JETP*, **56**, 322.
[53] BELYAKOV, V. A., DMITRIENKO, V. E., and ORLOV, V. P., 1980, *Sov. Phys. Usp.*, **22**, 63.
[54] BARBET-MASSIN, R., and PIERANSKI, P., 1984, *J. Phys. Lett.*, **45**, 799.
[55] BARBET-MASSIN, R., and PIERANSKI, P., 1985, *J. Phys., Paris*, **46**, C3,
[56] DOLGANOV, V. K., and VOITENKO, E. A., 1990, *Sov. Phys. Crystallogr.*, **34**, 265.
[57] FREIDZON, YA. S., TROPSCHA, YE. G., SHIBAEV, V. P., and PLATE, N. A., 1985, *Makromolek Chem. rap. Commun.*, **6**, 625.
[58] D'ALLEST, J., GILLI, J., and SIXOU, P., 1988, *Molec. Crystals liq. Crystals*, **155**, 571.
[59] STEGEMEYER, H., ONUSSEIT, H., and FINKELMANN, H., 1989, *Makromolec. Chem. rap. Commun.*, **10**, 571.
[60] DEMIKHOV, E. I., FREIDSON, YA. S., and SHIBAEV, V. P., 1989, *Vysokomol. Soedin.*, **31**, 3.
[61] DEMIKHOV, E., NIGGEMANN, E., and STEGEMEYER, H., 1992, *Phys. Rev.* A, **45**, 2380.
[62] NIGGEMANN, E., 1991, Thesis, Paderborn, p. 15.
[63] NICASTRO, A., and KEYES, P., 1983, *Phys. Rev.* A, **27**, 421.
[64] KEYES, P., NICASTRO, A., and MCKINNON, E., 1981, *Molec. Crystals liq. Crystals*, **67**, 715.
[65] BORN, M., 1972, *Optik* (Springer-Verlag), p. 403.
[66] HOHN, E., 1976, *Leitz Mitt. Wiss. Tech.*, **6**, 294.
[67] DMITRIENKO, V., 1989, *Liq. Crystals*, **5**, 847.
[68] PASTRNAK, J., and VEDAM, K., 1971, *Phys. Rev.* B, **3**, 2567.
[69] YU, P. Y., and CARDONA, M., 1971, *Solid. St. Commun.*, **9**, 1421.
[70] GINSBURG, V. L., 1958, *Sov. Phys. JETP*, **7**, 1096.
[71] LORENTZ, H. A., 1936, *Collected Papers*, **2**, 79; 1936, *Ibid.*, **3**, 14 (edited by M. Nijhoff, The Hague).
[72] CHEREPANOV, V. I., and GALISHEV, V. S., 1961, *Fiz. tverd. Tela*, **3**, 1085.
[73] TSEKAVA, V. E., 1961, *Sov. Phys. Solid State*, **3**, 847.
[74] AKOPIAN, R. S., ZELDOVICH, B. YA., and TABIRYAN, N. V., 1982, *Sov. Phys. JETP*, **56**, 1024.
[75] BELYAKOV, V. A., and DMITRIENKO, V. A., 1989, *Liq. Crystals*, **5**, 839.
[76] NYE, J. F., 1989, *Physical Properties of Crystals* (Oxford University Press), Chap. XIII.